Mechatronics, Electrical Power, and Vehicular Technology 05 (2014) 129-138

Mechatronics, Electrical Power, and Vehicular Technology

e-ISSN: 2088-6985
p-ISSN: 2087-3379
Accreditation Number: 432/Akred-LIPI/P2MI-LIPI/04/2012

www.mevjournal.com

AN EXPERIMENT OF OCULAR ARTIFACTS ELIMINATION FROM EEG SIGNALS USING ICA AND PCA METHODS

Arjon Turnip [a,*], Iwan R. Setiawan [a], Edy Junaidi [b], Le Hoa Nguyen [c]
[a]Technical Implementation Unit for Instrumentation Development,
Indonesian Institute of Sciences, Bandung, Indonesia
[b]Indonesian University of Education, Department of Physics, Bandung, Indonesia
[c]Dept. of Electrical Engineering, University of Science and Technology-The University of Danang, Vietnam.

Received 24 April 2014; received in revised form 10 November 2014; accepted 10 November 2014
Published online 24 December 2014

Abstract

In the modern world of automation, biological signals, especially Electroencephalogram (EEG) is gaining wide attention as a source of biometric information. Eye-blinks and movement of the eyeballs produce electrical signals (contaminate the EEG signals) that are collectively known as ocular artifacts. These noise signals are required to be separated from the EEG signals to obtain the accurate results. This paper reports an experiment of ocular artifacts elimination from EEG signal using blind source separation algorithm based on independent component analysis and principal component analysis. EEG signals are recorded on three conditions, which are normal conditions, closed eyes, and blinked eyes. After processing, the dominant frequency of EEG signals in the range of 12-14 Hz either on normal, closed, and blinked eyes conditions is obtained.

Keywords: EEG, EOG, ICA, PCA, artifacts elimination.

I. INTRODUCTION

The electrical activity produced by the brain is recorded by the electroencephalogram (EEG) using several electrodes placed on the scalp due to the effect of millions of neurons. Signals characteristics vary from one state to another, such as wakefulness/sleep or normal. Classically, five major brain waves can be distinguished by their frequency ranges: delta 0.5–4 Hz, theta 4–8 Hz, alpha 8–13 Hz, beta 13–30 Hz, and gamma 30–128 Hz [1].

The EEG has been developed in various fields such as the medical field, the development of Brain Computer Interface (BCI) [2-6], etc. In the medical field EEG is used to diagnose diseases such as epilepsy, metabolic encephalopathy, and cerebral parenchyma infective. Applications of EEG in the medical field are also able to determine the treatment to patients who have diseases related to nerves. In the development of BCI, EEG signals are used to move the cursor in two dimensions [7,8], to design a virtual keyboard [9,10], to move the three-dimensional simulations [11-14], and to design a mobile robot for users who have a physical or mental deficiency [2-4].

The recorded EEG signals are not only the original signal according to the brain activity but also contaminated by noise signals such as eye blink, eye movement, muscular movement, line noise, etc. [1,15-17]. Eye-blinks and movement of the eyeballs produce electrical signals that are collectively known as Ocular Artifacts (OA). The OA are pervasive problems in event-related potential (ERP) research.

The electric potentials created during saccades and blinks can be orders of magnitude larger than the EEG and can propagate across much of the scalp, masking and distorting brain signals. Therefore, these noise signals are required to be separated from the EEG signals to obtain the accurate results.

In a wide variety of research, artifact removal has been done by various methods. Signal recording method performed with a variety of stimulus, such as moving the limbs, moving the eyes, etc. Not only signal recording methods is

* Corresponding Author. Tel: +62-22-2503053
E-mail: jujhin@gmail.com

doi: 10.14203/j.mev.2014.v5.129-138

diverse, signal processing methods are also diverse. Among of them is independent component analysis (ICA) [15], principal component analysis (PCA) [18], adaptive filters, autoregressive models [19], non-liniear PCA [20], neural networks [21-25], wavelet denoising [1,15], gyroscope signal [16] etc. All of methods will be more powerfull when the artifacts are well identified.

This paper describes an experiment to identify the artifacts with completely automated method for eliminating electro ocular contamination from EEG signals using statistical criteria applied to data components obtained using a blind source separation (BSS) algorithm based on independent component analysis (ICA) and principal component analysis (PCA).

The artifact is composed of horizontal and vertical eye movements, and eye blinks as indicated in Table 1. In the experiment, the EEG signals when normal condition, closed eyes, and blinked eyes are recorded. ICA attempts to separate the EEG signals recorded into statistically independent sources (components), and then reject it with regard to artifacts. PCA is widely used for feature extraction by removing features that have no significant variance.

II. METHODS

This experiment involved seven male subjects with age range from 20 to 25 year old. All subjects had never done recording the EEG signals before. EEG signals were recorded using the Emotiv Epoch system (Figure 1(a)). EEG signals were recorded on a six channel is F7, F8, T7, T8, O1, and O2 as they relate to visual activity. Electrode placement pattern is shown in Figure 1(b).

Table 1.
Data recording scenarios

Time (second)	Stimulus	Activity
0-20	+	Normal
20-40	↓	Closed eyes
40-41	↑	Blinked eyes
41-45	+	Normal
45-46	↑	Blinked eyes
46-50	+	Normal
50-51	↑	Blinked eyes
51-55	+	Normal
55-56	↑	Blinked eyes
56-60	+	Normal

The first step of the experiment is the electrode preparation. Electrodes are firstly smeared using an electrolyte liquid to improve conductivity of the electrode. This process takes approximately 5 minutes, following by the pairing the Emotiv Epoch system on the subject and adjust the location of the electrodes on the scalp to record. Experiments carried out with three stimuli, i.e., normal conditions, closed eyes, and blinked eyes. Data recording scenarios is shown in Table 1.

Prior to ocular artifacts elimination using BSS based on ICA and PCA, a preprocessing operations filter FIR chebyshev type II was carried out. Flowchart of signals processing is shown in Figure 2.

A. Independent Component Analysis

ICA is one of algorithms group to solve the problem of blind source separation. Independent component analysis can be used to estimate a_{ij} based on independent information and this makes it possible to separate the original signals from their mixtures.

(a)

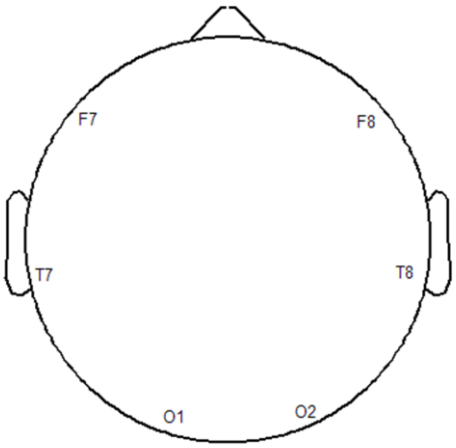

(b)

Figure 1. (a) Emotiv Epoch system; (b) Electrode placement pattern

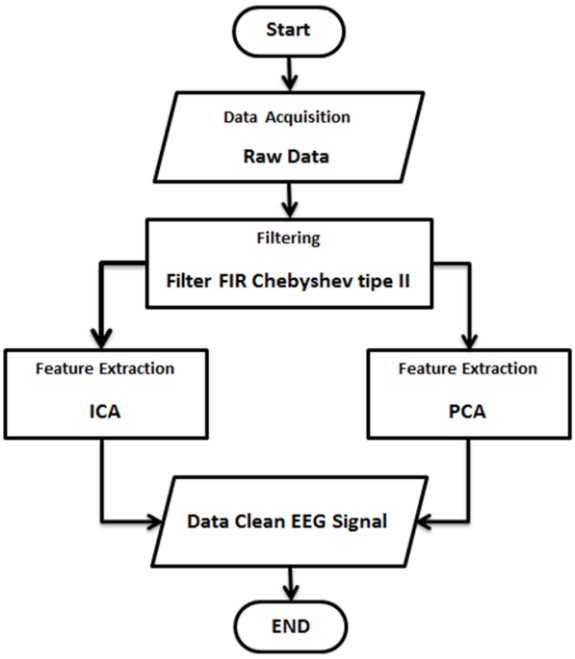

Figure 2. Flowchart of signals processing

The observed signal is denoted by x with elements $x_1, \ldots, x_n$, d and the original signal is denoted by s with elements $s_1, \ldots, s_n$, and A is the mixing matrix a_{ij}. With the vector notation, mixing models can be written as follows [20, 21]:

$$x = \mathrm{A}s \tag{1}$$

Estimating the independent components can be accomplished by finding the right linear combinations of the mixture variables, with invert the mixing as follow [20, 21]:

$$s = \mathrm{A}^{-1}x \tag{2}$$

thus, to estimate one of the independent components, we can consider a linear combination of the x_i. Assume a new vector as

$$y = b^T x = \sum b_i x_i \tag{3}$$

where b is a vector to be determined [20, 21].

$$\begin{aligned} y_1(t) &= b_{11}x_1(t) + b_{12}x_2(t) + b_{13}x_3(t) \\ y_2(t) &= b_{21}x_1(t) + b_{22}x_2(t) + b_{23}x_3(t) \\ y_3(t) &= b_{31}x_1(t) + b_{32}x_2(t) + b_{33}x_3(t) \end{aligned} \tag{4}$$

by substituting equation (1) to equation (3) it can be written $y = b^T\mathrm{A}s$. Thus, y is a certain linear combination of the s_i, where $b^T\mathrm{A}$ is a coefficient matrix denoted by q [20, 21]. So the equation (3) can be obtained

$$y = b^T x = q^T s = \sum q_i s_i \tag{5}$$

if b was one of the rows of the inverse of A, this linear combination $b^T x$ would actually equal one of the independent components. In that case, the corresponding q would be such that just one of its elements is 1 and the others are zero.

In practice, b and A cannot be determined but we can find an estimator that gives a good approximation. The fundamental idea here is that since a sum of two independent random variables is more Gaussian than the original variables, $y = q^T s$ is usually more Gaussian than any of the s_i and becomes the least Gaussian when it in fact equals to one of the s_i. In this case, obviously only one of the elements q_i of q is nonzero. In practice the values of q is unknown, but $q^T s = b^T x$ by the definition of q. Such a vector would necessarily correspond to a $q = \mathrm{A}^T b$, which has only one nonzero component. This means that $y = b^T x = q^T s$ equals to one of the independent components [20].

B. Principal Component Analysis

The starting point for PCA is a random vector x (i.e., $x(1), \ldots, x(T)$) with n elements. Typically the elements of x are measurements like pixel gray levels or values of a signal at different time instants. It is essential in PCA that the elements are mutually correlated, and there is thus some redundancy in xx. In the PCA transform, the vector x is first centered by subtracting its mean [20]:

$$x \leftarrow x - E\{x\} \tag{6}$$

The mean in this practice is estimated from the available sample $x(1), \ldots, x(T)$. Assume in the following that the centering has been done and thus $E\{x\} = 0$. Next, x is linearly transformed to another vector y with m elements ($m < n$) so that the redundancy induced by the correlations is removed. This is done by finding a rotated orthogonal coordinate system such that the elements of x in the new coordinates become uncorrelated.

At the same time, the variances of the projections of x on the new coordinate axes are maximized so that the first axis corresponds to the maximal variance, the second axis corresponds to the maximal variance in the direction orthogonal to the first axis, and so on. In mathematical terms, consider a linear combination [20, 21]:

$$y_1 = \sum_{k=1}^{n} w_{k1}x_k = {W_1}^T x, \tag{7}$$

where the vector x is the elements $x_1, \ldots, x_n$. The $w_{11}, \ldots, w_{n1}$ are scalar coefficients or weights of an n- dimensional vector W_1, and ${W_1}^T$ denotes the transpose of W_1. The factor y_1 is called the first principal component of x when the variance of y_1 is maximally large. Because of the variance

is depends on both the norm and orientation of the weight vector W_1, impose the constraint that in the norm of W_1 is constant become equal to 1 in practice. Thus we look for a weight vector W_1 maximizing the PCA criterion as follow

$$J_1^{PCA}(W_1) = E\{y_1^2\} = E\left\{\left(W_1^T x\right)^2\right\} = W_1^T E\{xx^T\}W_1 = W_1^T C_x W_1 \quad (8)$$

so that $\|W_1\| = 1$. The $E\{.\}$ is the expectation over the (unknown) density of input vector *x*. The matrix C_x is the *n* x *n* covariance matrix of *x* given for the zero-mean vector *x* with the correlation matrix as

$$C_x = E\{xx^T\} \quad (9)$$

It is well known from basic linear algebra that the solution to the PCA problem is given in terms of the unit-length eigenvectors $e_1, \ldots, e_n$ of the matrix C_x. The ordering of the eigenvectors is such that the corresponding eigenvalues $d_1, \ldots, d_n$ satisfy $d_1 \geq d_1 \geq \cdots \geq d_n$. The solution equation (8) is given by $W_1 = e_1$. Thus the first principal component of *x* is $y_1 = e_1^T x$.

The criterion J_1^{PCA} in equation (8) can be generalized to *m* principal components, with *m* any number between 1 and *n*. Denoting the *m*-th ($1 \leq m \leq n$) principal component by $y_m = W_m^T x$, with w_m the corresponding unit norm weight vector, the variance of y_m is now maximized under the constraint that y_m is uncorrelated with all the previously found principal components:

$$E\{y_m y_k\} = 0, k < m \quad (10)$$

note that the principal components y_m have zero means because of:

$$E\{y_m\} = E\{W_m^T x\} = 0 \quad (11)$$

The condition (10) yields:

$$E\{y_m y_k\} = E\{(W_m^T x)(W_k^T x)\} = W_m^T C_x W_k = 0 \quad (12)$$

For the second principal component, we have the condition as follow

$$W_2^T C W_1 = d_1 W_2^T e_1 = 0 \quad (13)$$

It is known that $W_1 = e_1$, thus looking for maximum variance $E\{y_2^2\} = E\{(W_2^T x)^2\}$ in the subspace orthogonal to the first eigenvector of C_x. The solution is given by $W_2 = e_2$. Likewise, recursively it follows that $W_k = e_k$. Thus the *k*-th principal component is $y_k = e_k^T x$.

III. RESULT

Preparatory to an analysis of the ocular elimination from EEG signals, actual signals were recorded in a six-channel (F7, F8, T7, T8, O1, and O2) configuration as they relate to visual activity. The raw data (see Figure 3) were first pre-processed using a filter FIR chebyshev type

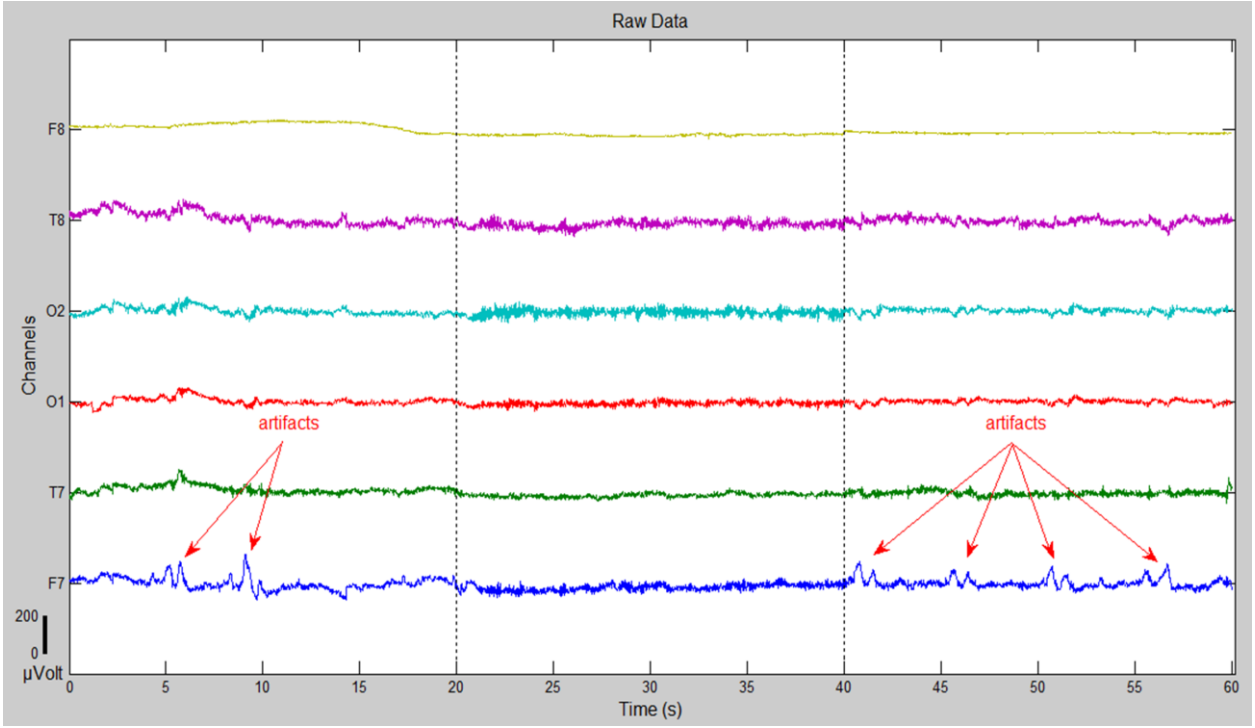

Figure 3. Recorded EEG Signal from the 1st subjects

II with cut-off frequencies of 0.5 (i.e., to remove the trend from low frequency bands) to 49 Hz (i.e., to remove unimportant information from high frequency bands), respectively (Figure 4). The low and the high frequency bands are clearly remove in Figure 4 compared to Figure 3 and the amplitude of EEG signals turn out to be 20-100 μV. All channels except channel F8 are highly contaminated by medium frequency bands.

It can be seen that the signals were corrupted by noises. Since the original EEG signal to the EEG power (noise) ratio is small, a method of extracting the brain activity component from the EEG is desirable. One way of gaining further

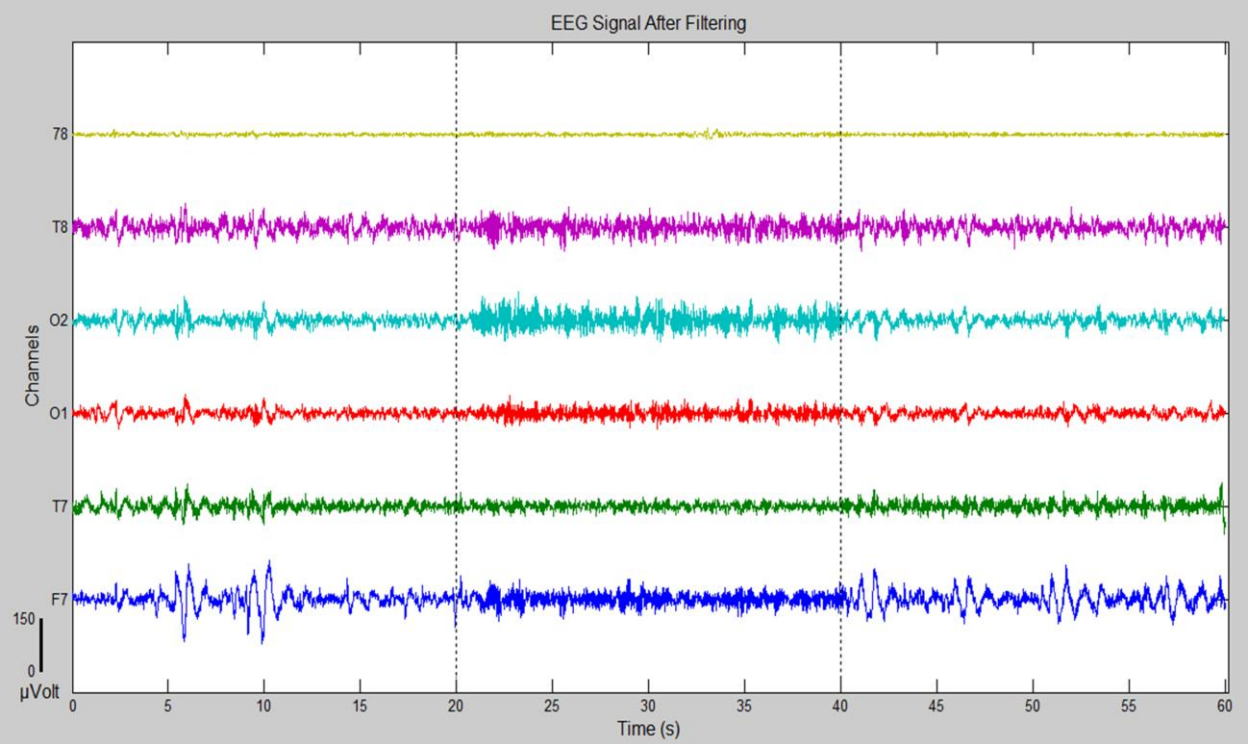

Figure 4. Filter EEG Signal using BPF

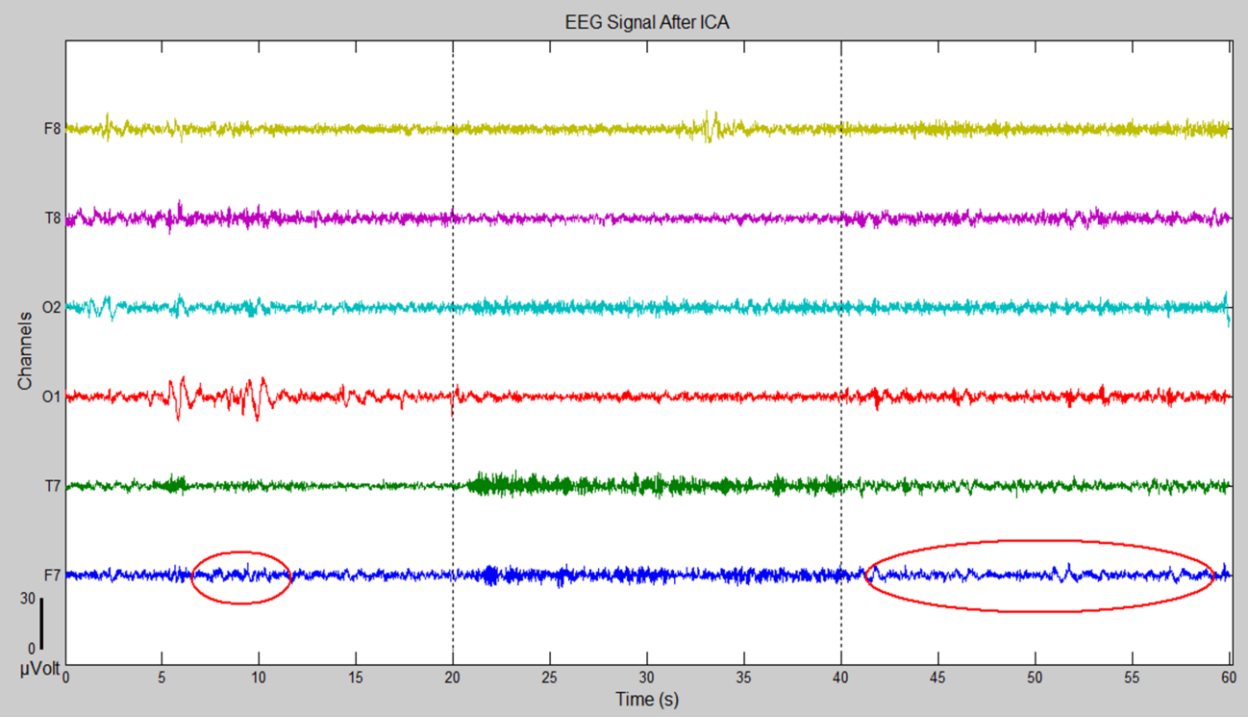

Figure 5. Clean EEG Signal using ICA

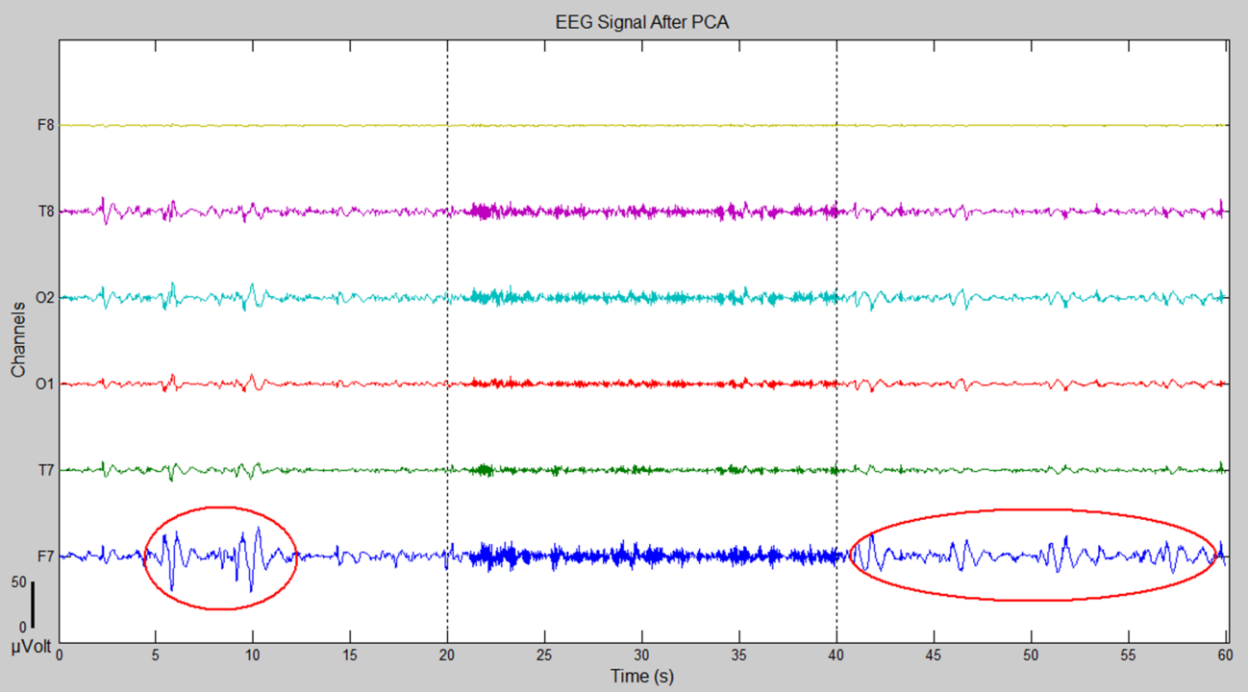

Figure 6. Clean EEG Signal using PCA

insights into EEG signals is by applying BSS based on ICA and PCA techniques. Figure 5 and Figure 6 shows the feature extraction results of the BSS base on ICA and PCA, respectively. The visually comparing the time domain plots, it is clear that the both algorithm reduces the amplitude of the ocular artifact while preserving the background EEG.

The extracted signals using both metods show the similarities of the signals propagation in each channel with the same condition of stimulus. The similarities patterns are given in the red color marks. In the closed eyes condition, the amplitude is a little bit higher compare with others condition. This results indicated that other conditions are more contaminated by noise. The other results about the highly degradation of the amplitude (from 100 μV to 10 μV) also indicated in the extracted EEG signals. Compared with the ICA method, the extracted EEG signals using PCA method produces EEG signals with larger amplitude as shown in Figure 6. This indicates that the signal is not completely separated from the mixture. Although the signals were still corrupted by noises (manifested as the high amplitudes of the artifacts in some sessions), the behaviors of the extracted signals clearly represented the brain activity components.

In order to show the visually performance of the extracted EEG signals, the brain mapping process is applied. The brain maps using both methods is given in Figure 7. The magnitude around 500 ms after given stimulus of each extracted signals are ploted in 2-D maps. The active brain regions that have been separated on any channels are indicated with a yellow to red. The red color indicated the higher brain activity and the blue color indicate the lower brain activity. The brain maps using PCA method indicates that the ocular artifacts are not perfectly separated (specially on channels F8 and O1) compared with the ICA method.

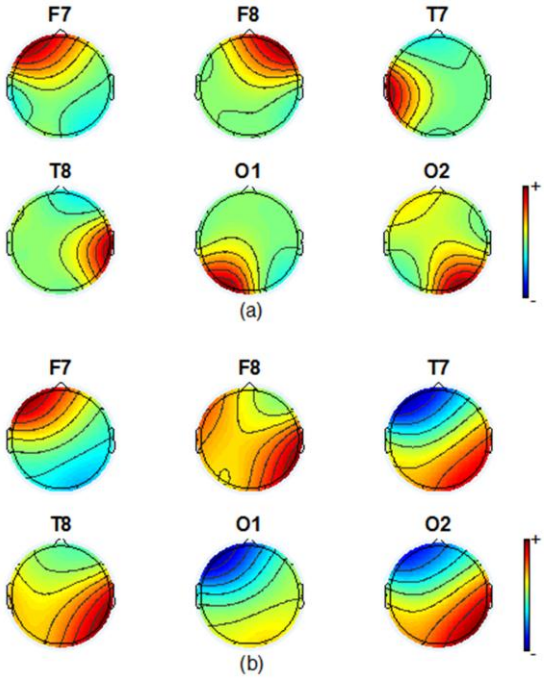

Figure 7. (a) Brain maps using ICA, (b) Brain maps using PCA

Other results about average EEG spectra based on three conditions stimulus (i.e. normal, closed, and blinked eyes condition) in the experiment using both methods are given in Figure 8 and Figure 9, respectively. The higher amplitude using both method is achieved in the range frequencies of 12-14 Hz. This results indicate that both method are success in eliminate the ocular artifacts without losing of important information on the recorded EEG signals.

The ICA method presents the amplitude: normal and blinked eyes condition about 1-1,5 μV while closed eyes condition about 5 μV. The PCA method present the amplitude: normal and blinked eyes condition about 1.3-1.4 μV while closed eyes condition about 18 μV. The differences in the level of amplitude between both methods indicate the ability of the separation of the noise from the brain activity in the recorded EEG signals. Dominant frequency

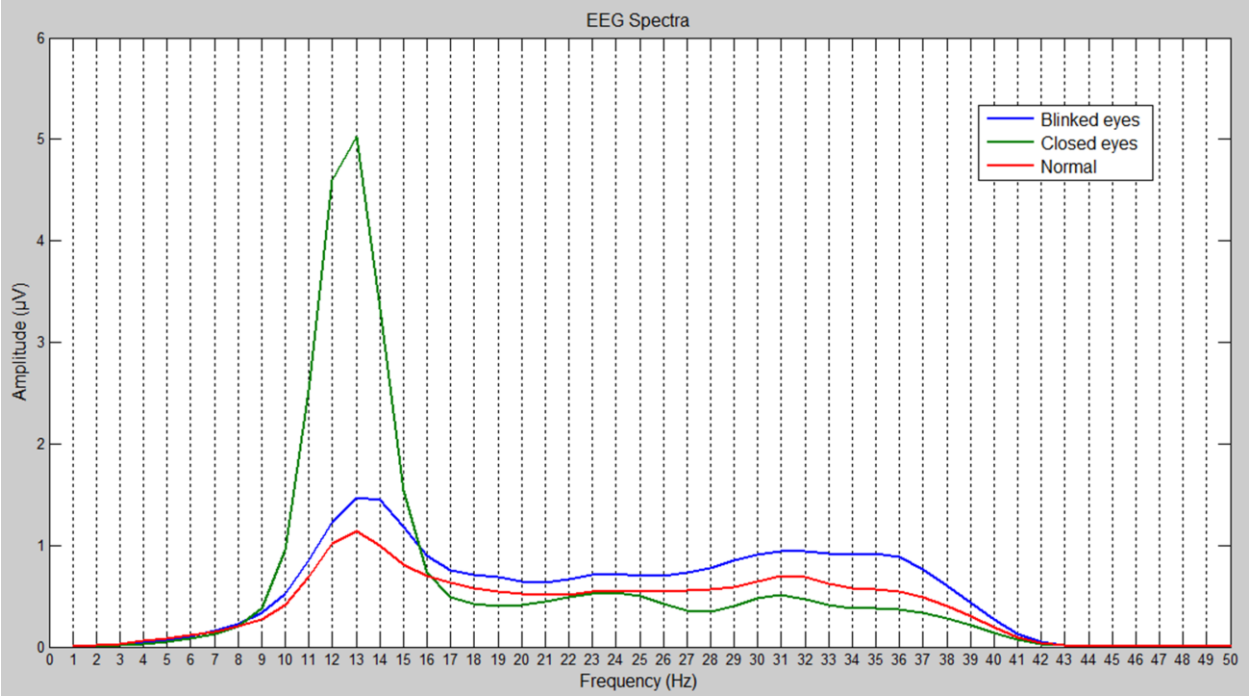

Figure 8. Average EEG spectra of each channels on normal, closed, and blinked eyes condition extracted using ICA

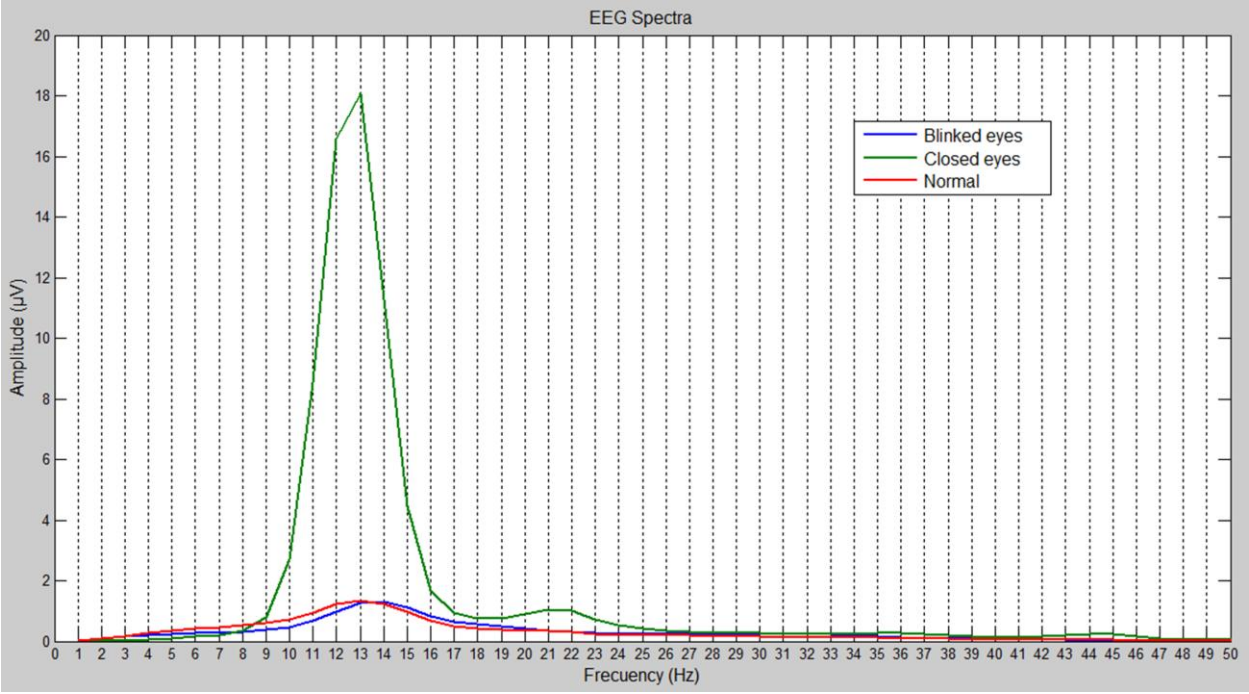

Figure 9. Average EEG spectra of each channels on normal, closed, and blinked eyes condition extracted using PCA

Table 2.
Frequency (Hz) and brainwave amplitude (μV) in normal, closed, and blinked eyes conditions using ICA

S	Normal		Closed Eyes		Blinked Eyes	
	F (Hz)	A (μV)	F (Hz)	A (μV)	F (Hz)	A (μV)
1	13	1,143	13	5,029	13	1,575
2	15	0,918	11	2,691	14	1,035
3	16	1,290	11	4,001	16	1,014
4	27	0,935	12	1,015	15	0,725
5	13	0,839	12	4,763	13	0,912
6	22	1,017	12	4,948	19	0,739
7	13	0,520	12	5,830	13	0,371

Table 3.
Frequency (Hz) and brainwave amplitude (μV) in normal, closed, and blinked eyes conditions using PCA

S	Normal		Closed Eyes		Blinked eyes	
	F (Hz)	A (μV)	F (Hz)	A (μV)	F (Hz)	A (μV)
1	13	1,355	13	18,087	14	1,318
2	14	1,603	11	6,488	13	2,326
3	16	0,468	12	2,721	12	0,312
4	13	1,496	12	9,911	13	1,323
5	12	4,144	12	14,899	12	3,063
6	11	0,475	12	14,538	9	0,465
7	12	4,296	12	17,706	12	4,070

and amplitude of each condition for all subjects are shown in Table 2 and Table 3 using ICA and PCA methods, respectively.

Table 2 and Table 3 show the brain waves spectrum of all subjects (S) in the frequency range about 11-16 Hz. There are two subjects with high frequency range under normal and blinked eyes conditions that are the 4^{th} and 6^{th} subject which is in the frequency range about 21-28 Hz. There are two possible reasons for these results: the subject was not focus on the given stimulus and or was not relaxed during the experiment. Overall results of the signal processing show the average frequency of normal condition, closed eyes, and blinked eyes more dominant in the frequency ranges of 12-14 Hz (alpha-beta). When the brain on alpha waves, it shows the subjects in a relaxed state, and beta waves showed that subjects in a state of full awareness, it is accordance with the current state of the recording signal. There are some subjects that have a larger frequency (high beta) than the other. When subjects are at high beta conditions, it indicate that the subjects were thinking on other activities or not to focus on the given stimulus.

IV. CONCLUSION

An experiment for the elimination of eye blink artifact from EEG signal using blind source separation algorithm based on independent component analysis and principal component analysis is reported. EEG signals are recorded on three conditions, which are normal conditions, closed eyes, and blinked eyes. After processing, the higher amplitude of EEG signals in the range of 12-14 Hz either on normal, closed, and blinked eyes conditions is obtained. Both methods are successfully eliminate the ocular artifacts without losing of important information on the recorded EEG signals.

ACKNOWLEDGMENT

This research was supported by the thematic program (No. 3425.001.013) through the Bandung Technical Management Unit for Instrumentation Development (Deputy for Scientific Services) and the competitive program (No. 079.01.06.044) through the Research Center for Metalurgy (Deputy for Earth Sciences) funded by Indonesian Institute of Sciences, Indonesia.

REFERENCES

[1] R. R. Vázquez, H. V. Pérez, R. Ranta, V. D. Louis, D. Maquin, and L. Maillard, "Blind source separation, wavelet denoising and discriminant analysis for EEG artefacts and noise cancelling," *Biomedical Signal Processing and Control*, vol. 7, pp. 389–400, 2012.

[2] L. Bi, X.-A. Fan, and Y. Liu, "EEG-Based Brain-Controlled Mobile Robots: A Survey," *IEEE Transactions On Human-Machine Systems*, vol. 43, no. 2, pp. 161-176, 2013.

[3] P. F. Dieza, S. M. T. Müller, V. A. Mut, E. Laciar, E. Avila, T. F. B. Filho, and M. S. Filho, "Commanding a robotic wheelchair with a high-frequency steady-state visual evoked potential based brain–computer interface," *Medical Engineering & Physics*, vol. 35, pp. 1155–1164, 2013.

[4] A. C. Lopes, G. Pires, and U. Nunes, "Assisted navigation for a brain-actuated intelligent wheelchair," *Robotics and Autonomous Systems*, vol. 61, pp. 245–258, 2013.

[5] A. Turnip, D. Soetraprawata, and D. E. Kusumandari, "A Comparison of EEG Processing Methods to Improve the Performance of BCI," *International Journal of Signal Processing Systems*, vol. 1, No. 1, 2013.

[6] A. Turnip, and D. E. Kusumandari, "Improvement of BCI performance through nonlinear independent component analisis extraction," *Journal of Computer*, vol. 9, no. 3, pp. 688-695, March 2014.

[7] B. Z. Allisona, C. Brunner, C. Altstätter, I. C. Wagner, S. Grissmann, and C. Neuper, "A hybrid ERD/SSVEP BCI for continuous simultaneous two dimensional cursor control," *Journal of Neuroscience Methods*, vol. 209, pp. 299– 307, 2012.

[8] Y. Li, J. Long, T. Yu, Z. Yu, C. Wang, H. Zhang, and C. Guan, "An EEG-Based BCI System for 2-D Cursor Control by Combining Mu/Beta Rhythm and P300 Potential," IEEE *Transactions On Biomedical Engineering*, vol. 57, no. 10, pp. 2495-2504, 2010.

[9] L. Mayaud, S. Filipe, L. Pétégnief, O. Rochecouste, and M. Congedo, "Robust Brain-computer Interface for virtual Keyboard (RoBIK): Project results" *IRBM*, vol. 34, pp. 131–138, 2013.

[10] R. B. Ashari, I. A. Al-Bidewi, and M. I. Kamel, "Design and simulation of virtual telephone keypad control based on brain computer interface (BCI) with very high transfer rates," *Alexandria Engineering Journal*, vol. 50, pp. 49–56, 2011.

[11] A. S. Royer, A. J. Doud, M. L. Rose, and B. He, "EEG Control of a Virtual Helicopter in 3-Dimensional Space Using Intelligent Control Strategies," *IEEE Transactions On Neural Systems And Rehabilitation Engineering*, vol. 18, no. 6, pp. 581-589, 2010.

[12] A. Akce, M. Johnson, O. Dantsker, and T. Bretl, "A Brain–Machine Interface to Navigate a Mobile Robot in a Planar Workspace: Enabling Humans to Fly Simulated Aircraft With EEG," *IEEE Transactions On Neural Systems And Rehabilitation Engineering*, vol. 21, no. 2, pp. 306-318, 2013.

[13] G. G. Gentiletti, J. G. Gebhart, R. C. Acevedo, O. Yáˇnez-Suárez, and V. Medina-Baˇnuelos, "Command of a simulated wheelchair on a virtual environment using a brain-computer interface," *IRBM*, vol. 30, pp. 218–225, 2009.

[14] H.-J. Hwang, K. Kwon, and C.-H. Im, "Neurofeedback-based motor imagery training for brain–computer interface (BCI)," *Journal of Neuroscience Methods*, vol. 179, pp. 150–156, 2009.

[15] G. Geetha, and S. N. Geethalakshmi, "Artifact Removal from EEG using Spatially Constrained Independent Component Analysis and Wavelet Denoising with Otsu's Thresholding Technique," *Procedia Engineering*, vol. 30, pp. 1064 –1071, 2012.

[16] S. O'Regan, S. Faul, and W. Marnane, "Automatic detection of EEG artefacts arising from head movements using EEG and gyroscope signals," *Medical Engineering & Physics*, vol. 35, pp. 867– 874, 2013.

[17] S. O'Regan, and W. Marnane, "Multimodal detection of head-movement artefacts in EEG," *Journal of Neuroscience Methods*, vol. 218, pp. 110–120, 2013.

[18] T. Liu, and D. Yao, "Removal of the ocular artifacts from EEG data using a cascaded spatio-temporal processing," *computer methods and programs in biomedicine*, vol. 83, pp. 95–103, 2006.

[19] V. Lawhern, W. D. Hairston, K. McDowell, M. Westerfield, and K. Robbins, "Detection and classification of subject-generated artifacts in EEG signals using autoregressive models," *Journal of Neuroscience Methods*, vol. 208, pp. 181–189, 2012.

[20] A. Cichocki and S.-I. Amari, Blind Decorrelation and SOS for Robust Blind Identification. Adaptive Blind Signal and Image Processing, Chapter 4, (2002).

[21] A. Turnip, K.-S. Hong, and M.-Y. Jeong, "Real-time feature extraction of P300 component using adaptive nonlinear principal component analysis," *Journal of BioMedical Engineering OnLine*, 10:83, 2011.

[22] D. Soetraprawata, and A. Turnip, "Autoregressive Integrated Adaptive Neural Networks Classifier for EEG-P300 Classification," *Journal of Mechatronics, Electrical Power and Vehicular Technology*, vol. 4, no. 1, pp. 1-8, 2013.

[23] H.-A. T. Nguyen, J. Musson, F. Li, W. Wang, G. Zhang, R. Xu, C. Richey, T. Schnell, F. D. McKenzie, and J. Li, "EOG artifact removal

using a wavelet neural network," *Neurocomputing*, vol. 97, pp. 374–389, 2012.

[24] A. Turnip, and D. Soetraprawata, "Performance of EEG-P300 Classification Using Backpropagation Neural Networks," *Journal of Mechatronics, Electrical Power and Vehicular Technology*, vol. 4, no. 2, pp. 81-88, 2013.

[25] A. Turnip, and K.-S. Hong, "Classifying mental activities from EEG-P300 signals using adaptive neural network," *International Journal of Innovative Computing, Information and Control* (IJICIC), vol. 8, no. 7, 2012.